Suplemento de la Revista Mexicana de Física **3** 0308007 (2022) 1–6

Results from low energy e^+e^- facilities of Budker Institute of Nuclear Physics

E. A. Kozyrev[a,b,*], F. V. Ignatov[a,b], R. R. Akhmetshin[a,b], A. N. Amirkhanov[a,b], A. V. Anisenkov[a,b], V. M. Aulchenko[a,b], N. S. Bashtovoy[a] , D. E. Berkaev[a,b], A. E. Bondar[a,b], A. V. Bragin[a], D. A. Epifanov[a,b], L. B. Epshteyn[a,b,c], A. L. Erofeev[a,b], G. V. Fedotovich[a,b], S. E. Gayazov[a,b], A. A. Grebenuk[a,b], S. S. Gribanov[a,b], V. L. Ivanov[a,b], S. V. Karpov[a], V. F. Kazanin[a,b], I. A. Koop[a,b], A. N. Kirpotin[b], A. A. Korobov[a,b], A. N. Kozyrev[a,c], P. P. Krokovny[a,b], A. S. Kuzmin[a,b], I. B. Logashenko[a,b], P. A. Lukin[a,b], K. Yu. Mikhailov[a], V. S. Okhapkin[a], Yu. N. Pestov[a], A. S. Popov[a,b], G. P. Razuvaev[a,b], Yu. A. Rogovsky[a,b], A. A. Ruban[a], N. M. Ryskulov[a], A. E. Ryzhenenkov[a,b], A. V. Semenov[a,b], Yu. M. Shatunov[a], P. Yu. Shatunov[a], V. E. Shebalin[a], D. N. Shemyakin[a,b], B. A. Shwartz[a,b], D. B. Shwartz[a,b], E. P. Solodov[a,b], V. M. Titov[a], A. A. Talyshev[a,b], A. I. Vorobiov[a], I. M. Zemlyansky[a], Yu. V. Yudin[a,b], V.P. Druzhinin[a,b], M.N. Achasov[a,b], A. Yu. Barnyakov[a], K. I. Beloborodov[a,b], A. V. Berdyugin[a,b], A. G. Bogdanchikov[a], A. A. Botov[a], T. V. Dimova[a,b], L. V. Kardapoltsev[a,b], A. G. Kharlamov[a,b], A. A. Korol[a,b], D. P. Kovrizhin[a], A. S. Kupich[a,b], N. A. Melnikova [a], A. E. Obrazovsky[a], E. V. Pakhtusova[a], K. V. Pugachev[a,b], S. I. Serednyakov[a,b], D. A. Shtol[a], Z. K. Silagadze[a,b], I. K. Surin[a], Yu. V. Usov[a], V. N. Zabin[a], V. V. Anashin[a], E. M. Baldin[a,b], A. Yu. Barnyakov[a,b], M. Yu. Barnyakov[a,b], S. E. Baru[a,b], I. Yu. Basok[a], E. A. Bekhtenev[a], O. V. Belikov[a], A. E. Blinov[a,b], V. E. Blinov[a,b], V. S. Bobrovnikov[a,b], A. V. Bogomyagkov[a,b], A. R. Buzykaev[a,b], S. I. Eidelman[a,b], D. N. Grigoriev[a,b,c], V. V. Kaminskiy[a,b], S. E. Karnaev[a], T. A. Kharlamova[a,b], V. A. Kiselev[a], S. A. Kononov[a,b], E. A. Kravchenko[a,b], V. N. Kudryavtsev[a,b], I. A. Kuyanov[a], V. M. Malyshev[a], A. L. Maslennikov[a], O. I. Meshkov[a,b], S. I. Mishnev[a], N. Yu. Muchnoi[a,b], D. A. Nikiforov[a], S. A. Nikitin[a], I. B. Nikolaev[a,b], I. N. Okunev[a], A. P. Onuchin[a,b], S. B. Oreshkin[a], V. V. Oreshonok[a], A. A. Osipov[a,b], I. V. Ovtin[a,b], A. V. Pavlenko[a], S. V. Peleganchuk[a,b], V. V. Petrov[a], P. A. Piminov[a], S. G. Pivovarov[a], N. A. Podgornov[a], V. G. Prisekin[a,b], O. L. Rezanova[a,b], G. A. Savinov[a], A. G. Shamov[a,b], L. I. Shekhtman[a], D. A. Shvedov[a], E. A. Simonov[a], S. V. Sinyatkin[a], A. V. Sokolov[a,b], E. V. Starostina[a,b], D. P. Sukhanov[a], A. M. Sukharev[a,b], A. A. Talyshev[a,b], V. A. Tayursky[a,b], Yu. A. Tikhonov[a,b], K. Yu. Todyshev[a,b], A. G. Tribendis[a], G. M. Tumaikin[a], Yu. V. Usov[a], V. N. Zhilich[a,b], A. A. Zhukov[a], V. V. Zhulanov[a,b], and A. N. Zhuravlev[a,b]

[a] *Budker Institute of Nuclear Physics, SB RAS.*
[*] *e-mail: e.a.kozyrev@inp.nsk.su*
[b] *Novosibirsk State University, Novosibirsk, 630090, Russia.*
[c] *Novosibirsk State Technical University, Novosibirsk, 630092, Russia.*

Received 15 January 2022; accepted 23 February 2022

The muon g-2 anomaly showing about 4σ deviation between the Standard Model (SM) prediction and the experiment is one of the most promising signals for physics beyond the SM. Also the hadronic uncertainties are limiting the accuracy of the SM prediction. We present the role of recent results, obtained with CMD-3, SND, and KEDR detectors at e^+e^- colliders VEPP-2000 (0.15÷1 GeV/beam) and VEPP-4M (1÷5 GeV/beam) in Novosibirsk, Russia, in improving the evaluations of hadronic vacuum polarization.

Keywords: Muon anomalous magnetic moment; g-2; e^+e^- annihilation; hadrons; non pertubative QCD; R measurement.

DOI: https://doi.org/10.31349/SuplRevMexFis.3.0308007

1. Introduction

We report recent results from the CMD-3, SND and KEDR detectors at the VEPP-2000 and VEPP-4M e^+e^- colliders in the Budker Institute in Novosibirsk. VEPP-2000 [1] and VEPP-4M [2] colliders were designed to operate in energies from 0.31 to 2.01 GeV and from 2 to 10 GeV in c.m.f., respectively.

A precise exclusive and inclusive measurement of the cross sections $e^+e^- \to hadrons$ is the most important part of our physics programme. In addition to the hadronic cross sections there is a long list of other interests. Two photon cross sections and transition form factors of C-even final systems can be measured in two fermion scattering method as well as in the direct two photon production without fermions in final state. Another two photon physics possibility arises from the radiative decay processes. Large focus of ongoing research belongs to the amplitude analyses, a study of internal dynamics of the hadronization process of an exclusive channels. One of the main features of Novosibirsk colliders is the possibility of precise energy determination with two methods: resonant depolarization method [3] and infrared light Compton backscattering method [4]. Budker institute facilities are able to make precise measurement of parameters of vector states ($J^{PC} = 1^{--}$) $\rho(770)$, $\omega(778)$, $\phi(1020)$ and its excited states, measurement of masses of mesons J/ψ, $\psi(2S)$, $\psi(3770)$, D^0, $D^{\pm}$, Υ(ns) and τ-lepton, measurement of total, leptonic and exclusive hadronic widths of charmonium like and other states.

The recently built injector delivers positrons to both experiments at VEPP-2000 and VEPP-4M colliders. The KEDR detector installed on the VEPP-4M is described in

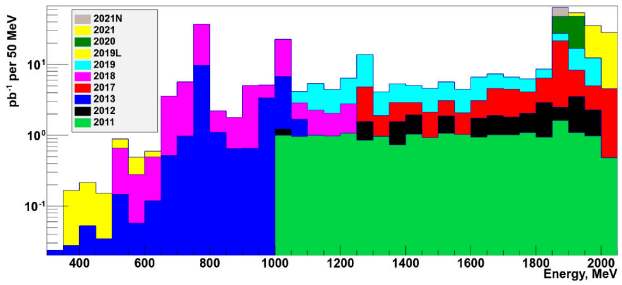

FIGURE 1. Distribution of the luminosity integral collected by CMD-3 detector up to date over the available VEPP-2000 energy range.

Ref. [5]. The VEPP-2000 provides a luminosity up to a half of $10^{32}\ 1/\mathrm{cm}^2/\mathrm{s}$ at a maximum center-of-mass energy from 160 MeV up to 2010 MeV. Two detectors, CMD-3 [6] and SND [7, 8], are installed in the two interaction regions. Both detectors have good energy and angular resolutions for charged particles and photons. The overall distribution of the collected luminosity integral over the VEPP-2000 energy range is shown in Fig. 1. At the beginning of the 2022 year, CMD-3 collaboration has collected about 400 1/pb overall. Increasing collected integral makes it interesting to search for rare decays like $\phi \to \pi^+\pi^-$, $\omega \to \pi^0\mu^+\mu^-$ and the decays of C-even mesons to hadrons, for example, $f_1(1285) \to \eta\pi^+\pi^-$ [9]. In this report, we present an overview of several specific results of data analysis.

Hadron production in the energy range s < 1 GeV is dominated by the $e^+e^- \to \pi^+\pi^-$ mode. This process gives the main contribution to the hadronic term of the anomalous magnetic moment of the muon g-2 and is crucial for its total theoretical precision. It is the most challenging channel because of a high-precision requirement on systematic uncertainties of 0.2% to complete new g-2 experiments and physics at future electron-positron colliders.

2. Measurement of the $e^+e^- \to \pi^+\pi^-$ cross section with SND detector

The measurement [10] is based on 4.6 pb^{-1} data collected in the energy range 0.53–0.88 GeV, about 10% of the full SND data set in this range. The event selection is based on excellent e/π separation provided by the three layer SND calorimeter. The measured $e^+e^- \to \pi^+\pi^-$ cross section is shown in Fig. 2 (left). The systematic uncertainty in the measurement is 0.8% in the energy range 0.6–0.9 GeV and 0.9% below 0.6 GeV. The curve in Fig. 2 (left) is the result of the fit to the data with the vector-meson-dominance (VMD) model including the $\rho(770)$, $\omega(782)$, and $\rho(1450)$ resonances. The model describes data well, the obtained resonance parameters are in reasonable agreement with the previous SND measurement [13] and the Particle Data Group Table [14]. Our measurements of the $e^+e^- \to \pi^+\pi^-$ cross section are in agreement with the previous energy-scan measurements performed at the VEPP-2M collider with the CMD-2 [15] and SND [13] detectors. The comparison of the fit to the SND data with the currently most accurate BABAR [16] and KLOE [17] measurements performed using the initial-state radiation technique is presented in Fig. 2 (middle and right). The systematic difference is observed between the SND and BABAR data below 0.7 GeV and between the SND and KLOE data above 0.7 GeV. The contribution to the muon anomalous magnetic moment from the $e^+e^- \to \pi^+\pi^-$ channel in the energy region 0.53–0.88 GeV calculated using the new SND data is $(409.8 \pm 1.4 \pm 3.9) \times 10^{-10}$. This value is in good agreement with the values obtained using the previous SND [13], BABAR [16], and KLOE [17] data.

3. Measurement of the $e^+e^- \to \pi^+\pi^-$ cross section with CMD-3 detector

The CMD-3 has plans to further reduce the systematic uncertainty achieved by CMD-2. Three energy scans below 1 GeV for the $\pi^+\pi^-$ measurement were performed at VEPP-2000 in 2013, 2018 and 2020. The collected data sample corresponds to about 64 pb^{-1} of integrated luminosity with 18 pb^{-1} during the first scan, 45 pb^{-1} during the second one and about 1 pb^{-1} during the last one. It is already higher than in any other experiments like previous CMD-2, the BaBar [16] and the KLOE [17] experiments (Fig. 3, left).

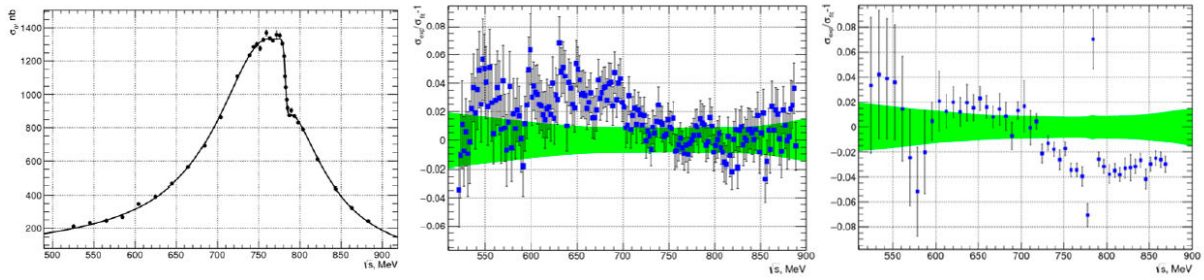

FIGURE 2. Left panel: The $e^+e^- \to \pi^+\pi^-$ cross section measured by SND. The curve is the result of the VMD fit. The relative difference between the BABAR [16] (middle panel) and KLOE [17] (right panel) $e^+e^- \to \pi^+\pi^-$ data and the SND fit. The band represents the statistical and systematic uncertainties of the SND fit combined in quadrature.

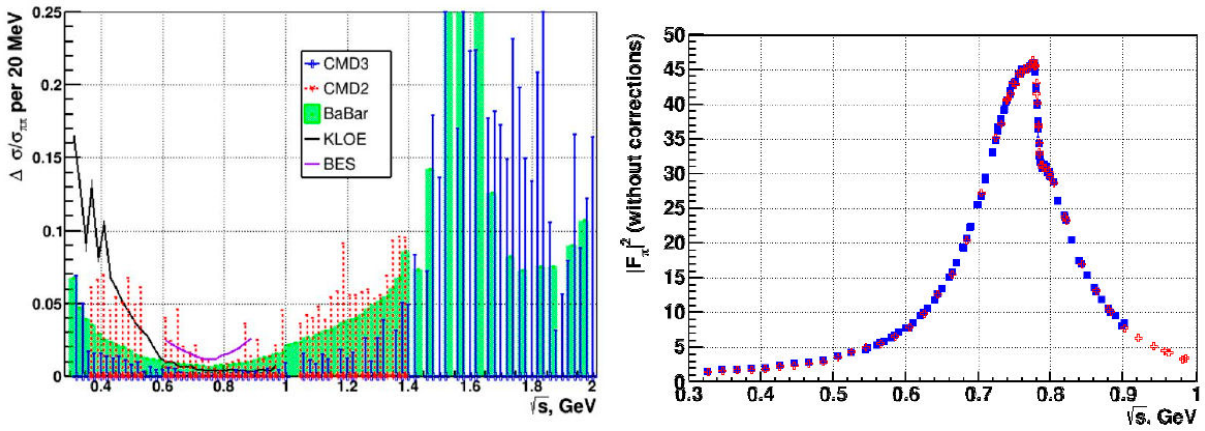

FIGURE 3. Left panel: Statistical precision of $|F_\pi|^2$ from the CMD-3 data collected during the 2013 and 2018 seasons in comparison with the results from CMD-2, BaBar, KLOE and BESIII. Right panel: Preliminary results on $|F_\pi|^2$ from CMD-3. Open crosses - separation done using the calorimeter information, filled squares - using particle momentum. Some additional corrections, common to two methods, are not applied.

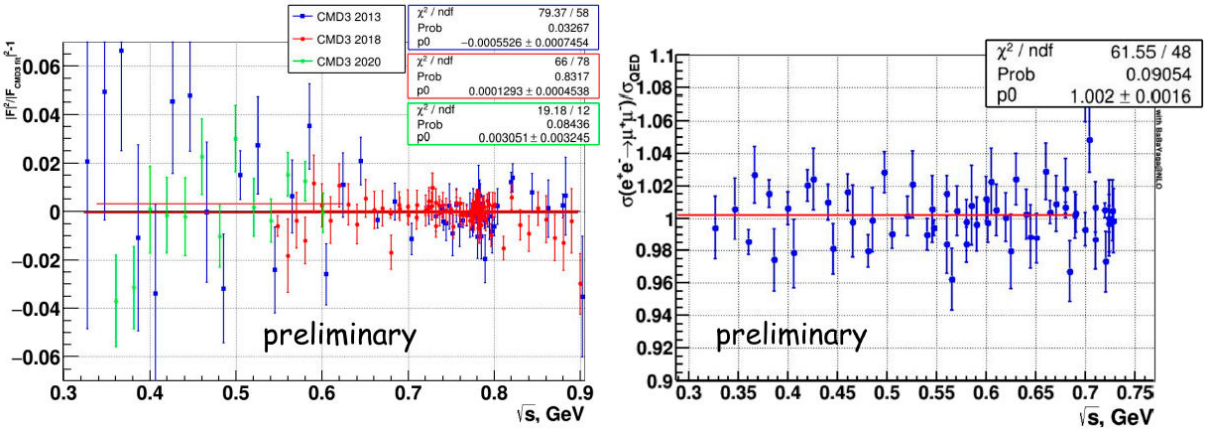

FIGURE 4. Left panel: Ratio of the measured 2π cross-section to the common fit $|F_\pi|^2$ parametrization. Right panel: Preliminary results of the measurement of muon pair production in comparison with the QED prediction.

The crucial pieces of analysis to reach the claimed goal include stable e/μ/π separation, precise fiducial volume determination, theoretical precision of radiative corrections, etc. An important point is that many systematic studies rely on high collected statistics. The $\pi^+\pi^-$ process has a simple event signature with two back-to-back charged particles. They can be selected by using the following criteria: two collinear well reconstructed charged tracks are detected, these tracks are close to the interaction point, both tracks are inside a good region of the drift chamber. The selected data sample includes events with e^+e^-, $\mu^+\mu^-$, $\pi^+\pi^-$ pairs and cosmic muons, and it practically does not contain any other physical background at energies $\sqrt{s} < 1$ GeV. These final states can be separated using either the information about energy deposition in the calorimeter or that about particle momenta in the drift chamber. At low energies the momentum resolution of the drift chamber is sufficient to separate different types of particles. The pion momentum is well aside from the electron one up to energies $\sqrt{s} = 0.9$ GeV, while the $\mu^+\mu^-$ events are separated from others up to $\sqrt{s} = 0.66$ GeV. At higher energies the peak of an electron shower in the calorimeter is far away from the peak of minimal ionization particles. Separation using energy deposition works better at higher energies and becomes less robust at lower energies. The preliminary result on the pion form factor measured by the CMD-3 is shown in Fig. 3 (right), comparing two approaches using either momentum information or energy deposition. The additional corrections, common to two methods (*e.g.*, the trigger efficiency), are not applied. These two methods overlap in the wide energy range and provide a cross-check of each other. Comparison of both methods is an important step before publishing first results. The comparison of results from three seasons of 2013, 2018 and 2020 is shown in Fig. 4 (left) (from the analysis based on momentum information). Good agreement is seen from the fits shown by the lines. One of the tests in this analysis is a measurement of the $e^+e^- \to \mu^+\mu^-$ cross section at low energy, where separation was performed using momentum information. Prelimi-

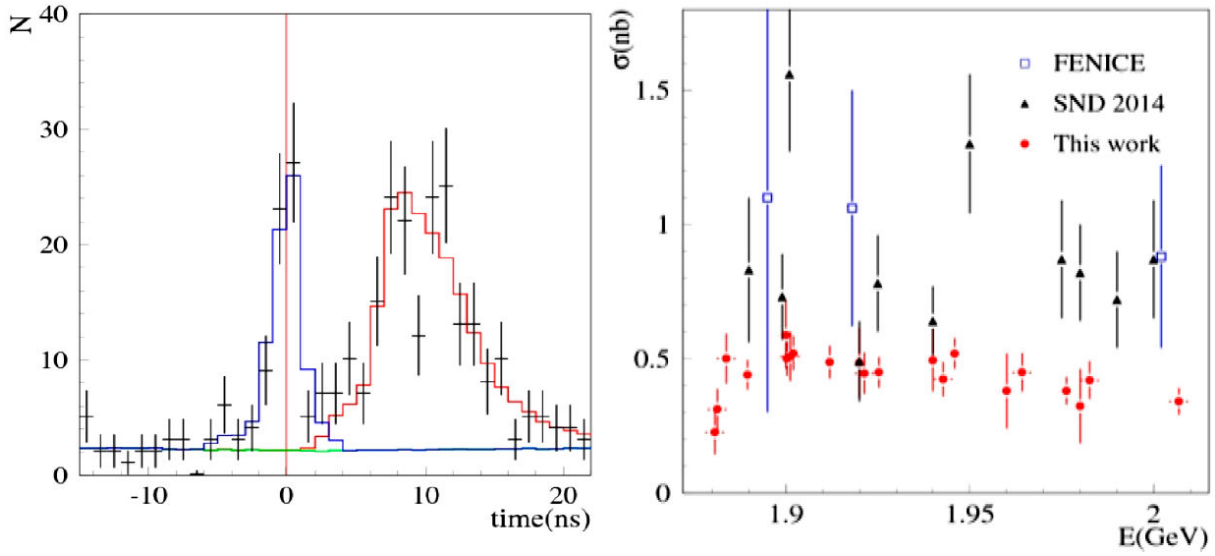

FIGURE 5. Left panel: The time distribution for selected data events collected in 2019 (points with error bars) at E=1.89 GeV. The blue histogram is the fitted total contribution of the cosmic-ray, beam-induced and physical backgrounds. The red histogram is the sum of the cosmic-ray background and fitted $n\bar{n}$ signal. Right panel: The preliminary SND results on the $e^+e^- \to n\bar{n}$ cross section (solid circles) compared with the previous FENICE [20] (empty squares) and SND [21] (filled triangles) measurements. Only statistical errors are shown.

nary results of this test are consistent with the QED prediction with an overall precision of 0.25% as shown in Fig. 4 (right). e/μ/π separation should be greatly improved with exploiting full power of the combined barrel calorimeter. The systematic contribution coming from the pion specific losses like nuclear interactions and decays in flight will be improved. Another important source of systematics is a theoretical precision of radiative corrections [19], which is mainly coming from the theoretical prediction of momentum spectra from differential cross sections. As seen from effects of two-photon contributions to momentum spectra, it becomes very desirable to have an exact NNLO $e^+e^- \to e^+e^-(\gamma\gamma)$ generator to reach precision $\leq 0.1\%$.

4. Study of the process $\mathbf{e^+e^- \to n\bar{n}}$

The process $e^+e^- \to n\bar{n}$ was previously measured by FENICE [20], and SND [21] using the 2011-2012 data set. The new SND measurement is based on 2017 and 2019 data and uses a different method of signal-background separation compared with Ref. [21].

For 2017 data, we analyze the distribution of the time difference between the calorimeter trigger and the beam revolution frequency. This difference is measured with a rather poor resolution of about 6 ns. In the 2019 run, the time measurement technique in the calorimeter was significantly improved [18]. For each calorimeter crystal, the signal from the photodetector shaped with an integration time of about 1 μs is digitized by a flash ADC with a sampling rate of 36 MHz. The signal amplitude and its arrival time are determined from the fit to the measured signal shape. The event time is calculated as a weighted average of crystal arrival times with the energy deposition used as a weight. The time resolution measured using $e^+e^- \to \gamma\gamma$ events is 0.8 ns, nearly an order of magnitude lower than that for the 2017 run.

The time distributions for selected data events of the 2019 run at $E = 1.89$ GeV and 1.95 GeV are shown in Fig. 5 (left). The time distribution consists of the nearly uniform cosmic-ray distribution, the distribution for the beam-induced and physical backgrounds, which is peaked near zero, and a wide $n\bar{n}$ distribution, which is shifted relative to other e^+e^- annihilation events due to small antineutron velocity. From the fit to data with the sum of the three distributions, we determine the number of $n\bar{n}$ events. Our preliminary results on the $e^+e^- \to n\bar{n}$ cross section are shown in Fig. 5 (right). The statistical accuracy of the measurement is significantly improved compared with the previous SND measurement [21]. However, the new SND result is lower than the previous one by about 30% at 1.9 GeV and by two times near 2 GeV. The main reasons are underestimated beam background and not quite correct MC simulation in the previous measurement. The systematic uncertainty on the cross section is estimated to be about 15%, mainly due to MC simulation.

The $e^+e^- \to n\bar{n}$ cross section depends on two form factors, magnetic and electric. The ratio of the form factors can be determined from the analysis of the antineutron polar angle distribution. The results of the fit to the angular distribution for the 2019 data set in three energy regions are listed in Table I. Our preliminary results agree with the assumption that $|G_E/G_M| = 1$, but also do not contradict larger values $|G_E/G_M| \approx 1.4$–1.5 observed in the BABAR [22] and BESIII [23] experiments for the ratio of proton form factors near $E = 2$ GeV.

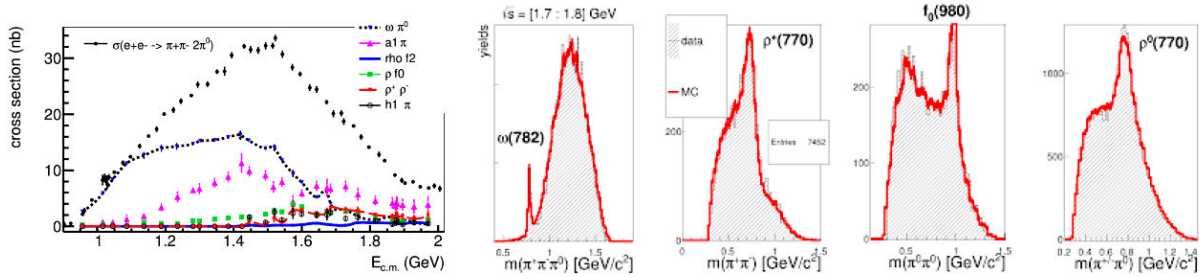

FIGURE 6. Left panel: Cross sections calculated for different components of the matrix element and the total $e^+e^- \to 2\pi^0\pi^+\pi^-$ cross section (black circles). Right panel: The data-MC comparison of the $\pi^+\pi^-\pi^0$, $\pi^+\pi^-$, $\pi^0\pi^0$ and $\pi^\pm\pi^0$ mass spectra for the process $e^+e^- \to \pi^+\pi^-2\pi^0$ in the energy range $\sqrt{s} = 1.7 \div 1.8$ GeV.

TABLE I. Preliminary SND results on the $|G_E/G_M|$ ratio.

Energy range (GeV)	1.89–1.902	1.91–1.925	1.95–1.975
$\lvert G_E/G_M\rvert$	0.77 ± 0.27	1.34 ± 0.33	1.70 ± 0.53

5. Other hadronic final states

5.1. $e^+e^- \to 4\pi$

Using the large data sample of $e^+e^- \to \pi^+\pi^-2\pi^0$ (64k events) and $e^+e^- \to 2\pi^+2\pi^-$ (72k events) collected by the CMD-3 the simultaneous analysis of these two final states was performed. Due to the limited detector acceptance the detection efficiency strongly depends on the production dynamics, which involves the mechanisms $\omega(782)\pi^0 \to \rho(770)2\pi^0$, $a_1\pi \to \rho(770)\pi$, $a_1\pi \to \sigma\pi\pi$, $h_1\pi \to \rho(770)2\pi$, $\rho(770)\rho(770)$, $\rho(770)f_0$ and others. To find the amplitudes of these mechanisms the unbinned fit of both $\pi^+\pi^-2\pi^0$ and $2\pi^+2\pi^-$ final states was done at each c.m. energy point. The contribution of each mechanism to the total hadronic current of the process was calculated using the effective lagrangian approach. The performed unbinned fit results are in a good data/Monte Carlo agreement for both final states, see Fig. 6 (right). Using the amplitudes obtained in the unbinned fit the contribution of each mechanism to the total cross section can be calculated (neglecting the interference), see Fig. 6 (left). More detalies about this analysis can be found in Ref. [24].

5.2. Nucleon antinucleon threshold

In 2017 the dedicated scan of energy range around $p\bar{p}$ and $n\bar{n}$ production thresholds was performed with small energy steps at VEPP-2000 collider. A very fast rise of $p\bar{p}$ cross section was observed [25] with width $\sim$1 MeV, consistent with the beam energy spread. A sharp drop at the same energies was observed for $e^+e^- \to 3(\pi^+\pi^-)$ and $e^+e^- \to K^+K^-\pi^+\pi^-$ cross sections. Observed behavior of the cross sections with a drop less than 2 MeV has similar origin, and can be explained by opening of the direct production of the nucleon antinucleon final state. Surprisingly, no narrow structure at $N\bar{N}$ threshold was observed for $e^+e^- \to \pi^+\pi^-\pi^+\pi^-$ cross section. We are planning to finish new data collection at $N\bar{N}$ threshold by the middle of 2022.

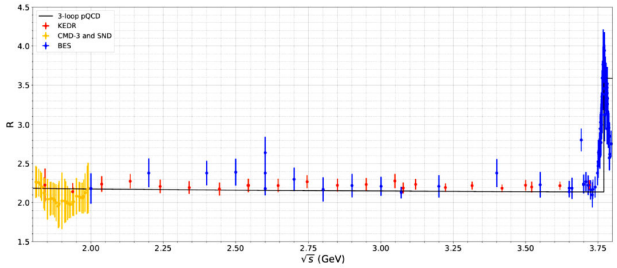

FIGURE 7. R measurement with KEDR detector between 1.8 and 3.8 GeV.

5.3. The measurement of R

In Fig. 7 the most recent measurements of R are presented in the energy range between 1.8 and 3.8 GeV in comparison with pQCD prediction. The J/ψ structure is omitted in the figure, while the right-side peak corresponds to the $\psi(2S)$ resonance opening the production of beauty hadrons. R was measured at KEDR in this energy range at 13 points between 1.84-3.05 GeV [11]. The achieved accuracy is about or better than 3.9% at the most of energy points. For the energies above J/ψ resonance there were 9 points with a total error of about or better than 2.6% [12]. The result is still consistent with the pQCD predictions within their errors.

New data taking was done in the energy range from 4.7 to 7 GeV with integrated luminosity 13.7 pb^{-1}. The range is interesting because there are no published data between 5 GeV and 6.96 GeV [22,23]. The VEPP-4M collected statistics at 17 equidistant points in this energy range. The total uncertainty is expected to be about 3% with systematical uncertainty of about 2.5%.

6. Summary

The VEPP-2000 collider delivered about 400 pb^{-1} of integrated luminosity in the energy range 0.32$\div$2.01 GeV to the

SND and CMD-3 detectors from 2010 to 2022. Today VEPP-2000 is the only one working on direct scanning of the region for measurement of exclusive values $\sigma(e^+e^- \to hadrons)$. The VEPP-2000 results will help to reduce the error of the hadronic contribution to vacuum polarization. Also our results are the independent cross-check of results from ISR processes, future precise Lattice QCD calculations, results on data in the space-like region.

The $e^+e^- \to \pi^+\pi^-$ and $e^+e^- \to n\bar{n}$ (preliminary) cross sections are measured with systematic uncertainty better then 1% and 10% respectively. Publication of a large number of precise measurements is expected soon. Data analysis for many hadronic final states is in progress. We have the goal to collect O(1) 1/fb at VEPP-2000 in 5 years, which should provide new precise results on the hadron production.

The most precise measurement of R was made between 1.84 and 3.72 GeV at the KEDR detector. Analysis of data in the energy range between 4.56 and 6.96 GeV was started, expected accuracy is less than 3%. New measuring of D-meson masses is ongoing with the aim to increase accuracy.

Acknowledgement

The work has been partially supported by the Russian Foundation for Basic Research grant No. 20-02-00496 A.

1. A. Romanov *et al.*, in *Proceedings of Particle Accelerator Conference PAC 2013, Pasadena, CA USA, 2013*, p. 14.
2. V. V. Anashin *et al.*, VEPP-4M Collider: Status and Plans, Proc. of EPAC 98*, Stockholm (1998) 400.
3. A. D. Bukin *et al.*, Absolute calibration of beam energy in the storage ring, Φ-meson mass measurement, Preprint IYF-75-64, 1975B.
4. G. Ya. Kezerashvili *et al.*, A Compton source of high-energy polarized tagged gamma-ray beams. The ROKK-1M facility, *Nucl. Instrum. Meth. B* 145 (1998) 40.
5. V. V. Anashin *et al.*, KEDR collaboration, The KEDR detector, *Phys. of Part. and Nucl.* **44** (2013) 657.
6. B.I. Khazin *et al.*, *Nucl. Phys .B, Proc. Suppl.* **376** (2008) 181.
7. A. Y. Barnyakov *et al.*, *JINST* **9** (2014) C09023.
8. V. M. Aulchenko *et al.*, *Nucl. Instrum. Methods Phys. Res., Sect. A* **598** (2009) 340.
9. M.N. Achasov *et al.* (SND Collaboration), *Phys. Lett. B* **800** (2020) 135074.
10. M. N. Achasov *et al.* (SND Collaboration), Measurement of the $e^+e^- \to \pi^+\pi^-$ process cross section with the SND detector at the VEPP-2000 collider in the energy region $0.525 < \sqrt{s} < 0.883$ GeV, *JHEP* **01** (2021) 113.
11. V.V. Anashin, *et al.*, KEDR collaboration, Measurement of R between 1.84 and 3.05 GeV at the KEDR detector, *Phys. Lett. B* 770 (2017) 174.
12. V.V. Anashin *et al.*, KEDR collaboration, Precise measurement of Ruds and R between 1.84 and 3.72 GeV at the KEDR detector, *Phys.Lett. B* **788** (2019) 42.
13. M. N. Achasov *et al.* (SND Collaboration), Update of the $e^+e^- \longrightarrow pi^+pi^-$ cross-section measured by SND detector in the energy region 400-MeV $<$ s**(1/2) $<$ 1000-MeV, *J. Exp. Theor. Phys.* **103** (2006) 380.
14. M. Tanabashi *et al.* (Particle Data Group), *Phys. Rev. D* **98** (2018) 010001.
15. R.R. Akhmetshin *et al.* (CMD-2 Collaboration), *Phys. Lett. B* **648** (2007) 28.
16. J. P. Lees *et al.* (BaBar Collaboration), Precise Measurement of the $e^+e^- \to \pi^+\pi^-(\gamma)$ Cross Section with the Initial-State Radiation Method at BABAR, *Phys. Rev. D* **86** (2012) 032013.
17. A. Anastasi *et al.* (KLOE Collaboration), *JHEP* **03** (2018) 173.
18. M. N. Achasov *et al.*, Time resolution of the SND electromagnetic calorimeter, *JINST*, **10** (2015) T06002.
19. S. Actis *et al.*, *Eur. Phys. J. C* **66** (2010) 585.
20. A. Antonelli *et al.* (FENICE Collaboration), The first measurement of the neutron electromagnetic form-factors in the time-like region, *Nucl. Phys. B* **517** (1998) 3.
21. M. N. Achasov *et al.* (SND Collaboration), Study of the process $e^+e^- \to n\bar{n}$ at the VEPP-2000 e^+e^- collider with the SND detector, *Phys. Rev. D* **90** (2014) 112007,
22. J. P. Lees *et al.* (BaBar Collaboration), Study of $e^+e^- \to p\bar{p}$ via initial-state radiation at BABAR, *Phys. Rev. D* **87** (2013) 092005.
23. M. Ablikim *et al.* (BESIII Collaboration), Measurement of proton electromagnetic form factors in $e^+e^- \longrightarrow p\bar{p}$ in the energy region $2.00 - 3.08$ GeV, *Phys. Rev. Lett.* **124** (2020) 042001.
24. E.A. Kozyrev *et al.*, *EPJ Web Conf.*, **212** (2019) 03008.
25. R. R. Akhmetshin *et al.*, *Phys. Lett. B* **794** (2019) 64.